Structure and Reactivity of Diamidoiron(III) Hydroperoxide. The Mechanism of Oxygen Atom Transfer to Ammonia

Robert D. Bach,* Ming-Der Su, José L. Andrés,† and H. Bernhard Schlegel

Contribution from the Department of Chemistry, Wayne State University, Detroit, Michigan 48202

Received November 22, 1991®

Abstract: Diamidoiron(III) hydroperoxide has been examined as a highly simplified model for the hydroperoxide intermediate in hemoproteins such as peroxidases and cytochrome P-450. Equilibrium structures and transition states were optimized at the UHF and UMP2 levels using the 3-21G basis and the Wachters–Hay basis set (augmented with an f function on iron). The MP2 level was found to be essential for a proper description of the geometry and bonding. Diamidoiron(III) hydroperoxide is a peroxo-bridged structure with Fe–O bond lengths of 1.98 and 2.15 Å. A CASSCF/3-21G geometry optimization also afforded a cyclic Fe–OOH structure with an Fe–O–O bond angle of 70.4°. Similar calculations on $(HO)_3TiOOH$ yielded a bridged structure in excellent agreement with X-ray data. The barrier for oxygen transfer from diamidoiron(III) hydroperoxide to ammonia is only 10.2 kcal/mol (MP4 energies using the Wachters–Hay basis), a barrier lower than that for LiOOH (20.0 kcal/mol) and peroxyformic acid (17.8 kcal/mol). Protonated diamidoiron(III) hydroperoxide is no longer bridged (R(Fe–O) = 2.01 and 2.85 Å) and has a negative barrier for oxygen donation to NH_3. Although these highly abbreviated models have many shortcomings, the present calculations suggest that in certain cases oxygen atom transfer from iron hemoproteins could precede the formation of the ferryl complex.

Introduction

Hemoproteins possess novel catalytic properties in the activation of dioxygen and play a unique role in biochemistry. The diversity of substrates and the variety of transformations that these enzymes execute crosses many fields of chemistry.[1] The role of porphyrin intermediates such as peroxidases and cytochrome P-450 has elicited much conjecture regarding the actual structure of the oxygen atom donor.[2] Despite the fact that the active oxygen species has never been isolated or characterized, there is almost universal acceptance that a ferryl (Fe=O) complex is involved in the enzymatic cycle that transfers a single oxygen atom to the substrate.[1,2] This putative monooxygen iron(V) oxygen donor can be derived in principle from an iron(III) hydroperoxide intermediate in a catalytic process by the loss of water (eq 1).

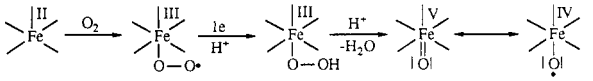

(1)

High-valent iron–oxo intermediates are also increasingly implicated in dioxygen activation by non-heme iron enzymes.[3] The assumption that O–O bond cleavage precedes the oxygen-transfer step has also influenced the design of metal complexes which mimic active sites in functional metalloproteins, and these studies have also been directed toward monooxygen intermediates. The first suggestion to the contrary has recently appeared,[3] where an $Fe^{III}OOH$ intermediate has been invoked in a P-450 dependent C–C bond cleavage.

The reactions of hydrogen peroxide with peroxidases and catalase also result in heterolytic cleavage of the oxygen–oxygen bond to produce an oxene intermediate (eq 2). Crystal structures

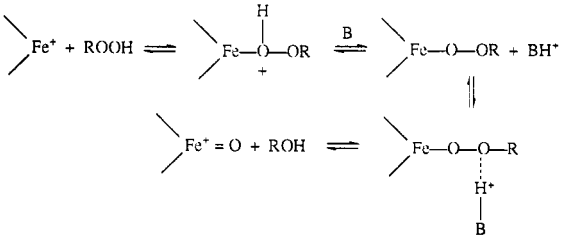

(2)

of cytochrome c peroxidase and catalase support general acid/general base involvement in assisting the hydroxide group to leave the iron hydroperoxide intermediate.[4] One of the fundamental questions that must be addressed when considering the mechanism for oxygen transfer from a hydroperoxide is the position of the proton in the transition state. A simplified version of the equilibrium involved in eq 2 is sometimes written as

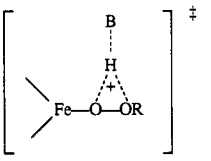

The concept of a ferryl (Fe=O) intermediate in P-450 catalyzed and related oxygenations is generally accepted, and most theoretical studies have been directed toward model ferryl compounds. Very little consideration has been given to hydroperoxide precursors of these ferryl oxygen donors.[5] A variety of semiempirical quantum calculations have described such model heme complexes.[5a–c] *Ab initio* calculations have studied the relative stability of oxygen-bridged iron and porphine nitrogen[5d,e] and the mechanism of alkene epoxidation,[5f] while a CASSCF study[5g] has described the electronic nature of the Fe=O bond.

† Universitat Autonoma Barcelona, Departamento de Quimica, 08193 Bellaterra, Catalonia, Spain.

® Abstract published in *Advance ACS Abstracts,* September 1, 1993.

(1) (a) *Cytochrome P-450: Structure, Mechanism and Biochemistry*; Ortiz de Montellano, P. R., Ed.; Plenum Press: New York and London, 1986. (b) McMurry, T. J.; Groves, J. T. *Ibid.* 1986; p 1.

(2) (a) Guengerich, F. P.; MacDonald, T. L. *Acc. Chem. Res.* **1984**, *17*, 9. (b) Groves, J. T.; Watanabe, Y. *J. Am. Chem. Soc.* **1986**, *108*, 507, 7834. (c) Traylor, T. G.; Xu, F. *J. Am. Chem. Soc.* **1990**, *112*, 178. (d) Zipplies, M. F.; Lee, W. A.; Bruice, T. C. *J. Am. Chem. Soc.* **1986**, *108*, 4433.

(3) Corina, D. L.; Miller, S. L.; Wright, J. N.; Akhtar, M. *J. Chem. Soc., Chem. Commun.* **1991**, 782.

(4) (a) Poulas, T. L.; Kraut, J. *J. Biol. Chem.* **1980**, *255*, 8199. (b) Vainshtein, B. K.; Melik-Adamyan, W. R.; Barynin, V. V.; Vagin, A. A.; Grebenko, A. I.; Borisov, V. U.; Bartels, K. S.; Fita, I.; Rossmann, M. G. *J. Mol. Biol.* **1986**, *88*, 49.

0002-7863/93/1515-8763$04.00/0

There have been no high-level *ab initio* calculations on an iron-(III) hydroperoxide. We now report the electronic structure of a peroxo-bridged iron(III) hydroperoxide and its transition structure for the oxidation of ammonia where transfer of the oxygen atom occurs in concert with O–O bond cleavage.

Method of Calculation

Molecular orbital calculations were carried out using the Gaussian 92 program system[6a] by utilizing gradient geometry optimization.[6b] The geometries of the reactants and transition structures that do not contain iron were first determined at the Hartree–Fock (HF) level of theory with the 3-21G and 6-31G* basis sets. All geometries were then fully optimized using second-order Møller–Plesset perturbation theory (MP2/6-31G*). Relevant energies and barrier heights were computed with the 6-31G* basis set using fourth-order Møller–Plesset perturbation theory (frozen core, MP4SDTQ/6-31G*//MP2/6-31G*). Vibrational frequency calculations at the MP2/6-31G* level were used to characterize the lithium-containing compounds as either minima (zero imaginary frequencies) or first-order transition states (a single imaginary frequency).

The iron hydroperoxides were initially optimized with the 3-21G basis set at both the HF and MP2 levels. The metal atoms basis sets are the 3-21G basis set reported by Hehre and [8s, 6p, 2d] contraction of the (14s, 11p, 5d) primitive set of Wachters.[8a] The Hay diffuse function[8b] and a 1-G 4f polarization function (exponent = 1.339)[8c] are added to the valence shell. The basis set in this form has 48 basis functions per metal atom and is referred to as the WH basis set. The O, N, and H basis sets are the 3-21G and the double-ζ Huzinaga–Dunning[8d,e] supplemented with d functions on N and O. Iron hydroperoxide **7** and its transition state (TS-8) for the oxidation of ammonia were fully optimized with the WH basis set. A frequency calculation using analytical second derivatives at the HF/WH level established **7** to be a true minimum. The MP4 correlation correction used the frozen core approximation with 13 and 14 core and virtual orbitals frozen in **7** and TS-8, respectively.

Results and Discussion

1,2-Hydrogen Shifts in Hydrogen Peroxide Cations. One of the generally accepted mechanistic features of oxygen atom transfer from a hydroperoxide is that a 1,2-hydrogen shift occurs in concert with nucleophilic attack by the substrate (eq 3). Recent

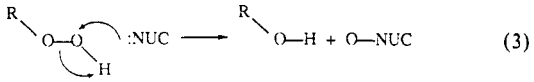

(3)

ab initio calculations[9a,d] predict that the hydrogen-transfer component must occur either prior to or after the oxygen transfer because of the prohibitively high activation barrier associated with a concerted 1,2-hydrogen shift in a hydrogen peroxide. The barrier height for conversion of hydrogen peroxide to water oxide (eq 4) is 53.4 kcal/mol at the MP4SDTQ/6-31G*//MP2/6-31G* level of theory. Of equal importance to the present study, the barrier for reversion of water oxide **2** to hydrogen peroxide is only 3.7 kcal/mol.[10] Water oxide is also predicted to exist as a stable minimum at the CCSD/TZ2p+f level with $\Delta E_2^{\ddagger}$ = 3.2 kcal/mol.[11] The barrier for a concerted 1,2-hydrogen shift in a metal-complexed hydroperoxide is of relevance to the overall mechanistic picture for peroxidases (eq 2).

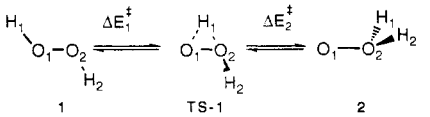

(4)

We initiated this study with the degenerate rearrangement of protonated hydrogen peroxide (Figure 1). The barrier heights for the 1,2-hydrogen shift in cation **3** are predicted to be 34.1 and 43.3 kcal/mol for the trans (TS-2) and cis (TS-3) pathways, respectively (Figure 2). The higher energy for the cis transition structure reflects the eclipsed hydrogens and the increased oxygen lone pair repulsion.

We have found that using a lithium cation as a substitute for heavier metals in preliminary studies is a useful protocol that provides us with mechanistic insight and reduces overall computational time. In principle, protonation of lithium hydroperoxide (LiOOH) can afford lithium hydrogen peroxide cation (**5**) or lithium water oxide cation (**6**) (Figure 3). The hydrogen peroxide cation **5** is 26.0 kcal/mol lower in energy than its isomeric water oxide cation **6**, reflecting the destabilizing influence of the dipolar isomer of hydrogen peroxide. Lithium cation **5** can also arise in solution from the complexation of hydrogen peroxide with lithium cation.

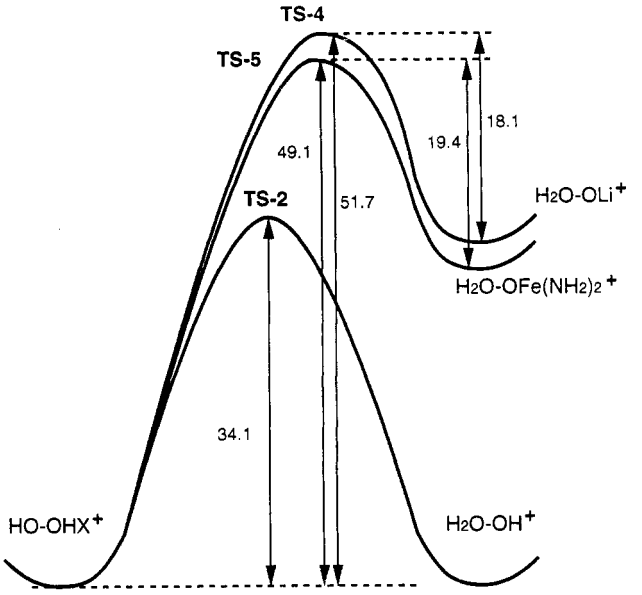

Figure 1. Energy profies for the 1,2-proton transfer in the protonated hydrogen peroxide (TS-2, X = H, MP4//MP2/6-31G*), lithium hydrogen peroxide (TS-4, X = Li, MP4//MP2/6-31G*), and diamidoiron hydrogen peroxide (TS-5, X = $Fe(NH_2)_2$, MP2/6-31G*).

(5) (a) Loew, G. H. In *Iron Porphyrin*; Lever, A. B. P.; Gray, B., Eds.; Addison-Wesley: Reading, MA, 1983, Part 1, pp 1–87. (b) McLean, A. D. *J. Am. Chem. Soc.* **1990**, *112*, 8686. (c) Edwares, W. D.; Zerner, M. C. *Theor. Chim. Acta* **1987**, *72*, 347. (d) Strich, A.; Veillard, A. *Theor. Chim. Acta* **1981**, *60*, 379; *Nouv. J. Chim.* **1983**, *7*, 347. (e) Yamaguchi, K.; Takahara, Y.; Fueno, T. In *Applied Quantum Chemistry*; Smith, V. H., Schaefer, H. F., Morokuma, K., Eds.; Reidel: Dordrecht, The Netherlands, 1986; p 155. (f) Yamamoto, S.; Teraoka, J.; Kashiwagi, H. *J. Chem. Phys.* **1988**, *88*, 303. (g) Yamamoto, S.; Kashiwagi, H. *Chem. Phys. Lett.* **1989**, *161*, 85; **1988**, *145*, 111.

(6) (a) Frisch, M. J.; Trucks, G. W.; Head-Gordon, M.; Gill, P. M. W.; Wong, M. W.; Foresman, J. B.; Johnson, B. G.; Schlegel, H. B.; Robb, M. A.; Replogle, E. S.; Gomperts, R.; Andres, J. L.; Raghavachari, K.; Binkley, J. S.; Gonzalez, C.; Martin, R. L.; Fox, D. J.; Defrees, D. J.; Baker, J.; Stewart, J. J. P.; Pople, J. A. GAUSSIAN 92, Gaussian, Inc., Pittsburgh, PA, 1992. (b) Schlegel, H. B. *J. Comput. Chem.* **1982**, *3*, 214.

(7) Dobbs, K. D.; Hehre, W. J. *J. Comput. Chem.* **1987**, *8*, 861.

(8) (a) Wachters, A. J. H. *J. Chem. Phys.* **1970**, *52*, 1033. (b) Hay, J. P. *Ibid.* **1977**, *66*, 4377. (c) Stewart, R. F. *Ibid.* **1970**, *52*, 431. (d) Huzinaga, S. *Ibid.* **1965**, *42*, 1293. (e) Dunning, T. H. *Ibid.* **1970**, *53*, 2823.

(9) (a) Bach, R. D.; Owensby, A. L.; Andrés, J. L.; Schlegel, H. B. *J. Am. Chem. Soc.* **1991**, *113*, 7031. (b) Bach, R. D.; Wolber, G. J.; Coddens, B. A. *J. Am. Chem. Soc.* **1984**, *106*, 6098. (c) Bach, R. D.; Owensby, A. L.; González, C.; Schlegel, H. B.; McDouall, J. J. W. *Ibid.* **1991**, *113*, 6001. (d) Bach, R. D.; Owensby, A. L.; González, C.; Schlegel, H. B. *J. Am. Chem. Soc.*, submitted for publication.

(10) With full geometry optimization, the QCISD(T) barrier for $\Delta E_1^{\ddagger}$ = 51.4 kcal/mol while $\Delta E_2^{\ddagger}$ = 3.2 kcal/mol, unpublished results.

(11) Meredith, C.; Hamilton, T. P.; Schaefer, H. F., III *J. Phys. Chem.* **1992**, *96*, 9250.

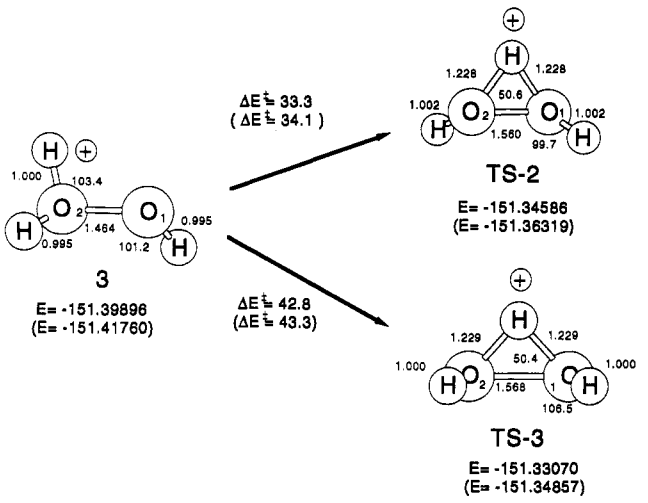

Figure 2. Optimized geometries for protonated hydrogen peroxide (3) and the transition structures for a 1,2-hydrogen shift in the trans conformation (TS-2) and cis conformation (TS-3) at the MP2/6-31G* level. Distances are given in Å, angles in deg, relatives energies in kcal/mol, and total energies in au (MP4//MP2/6-31G* energies in parentheses).

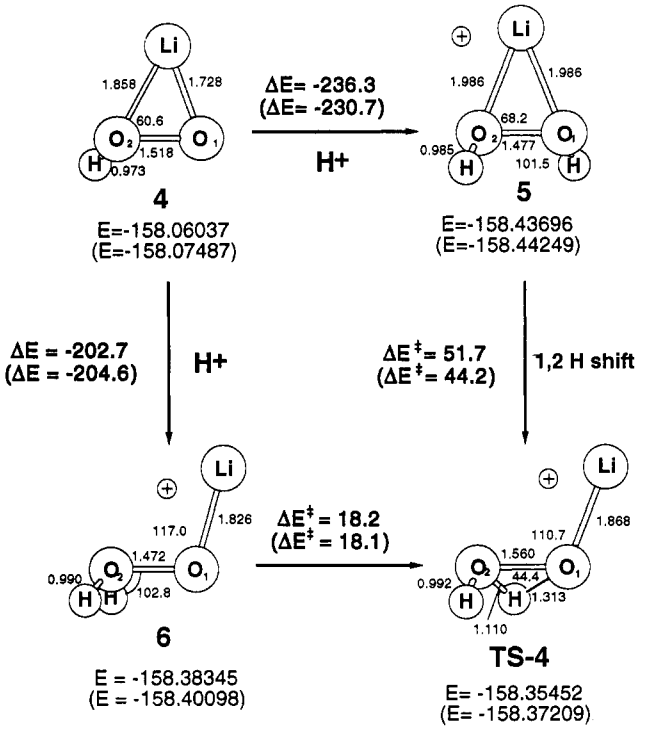

Figure 3. 1,2-Hydrogen shifts in the lithium hydrogen peroxide cation calculated at MP2/6-31G* and MP4//MP2/6-31G* (in parentheses). Distances are given in Å, angles in deg, total energies in au, and relative energies in kcal/mol.

In solution the interconversion of lithium cations **5** and **6** would almost certainly proceed by a protonation–deprotonation process since the gas-phase activation barrier for a concerted 1,2-hydrogen shift (TS-4) is calculated to be 44.2 kcal/mol. Significantly, the lithium cation of water oxide lies in a potential well (Figure 1) that is predicted to be 18.1 kcal/mol below TS-4 (Figure 3), suggesting that this cation could have a sufficient lifetime to be a potential oxygen atom donor. As noted above, the activation barrier for reversion of the high energy water oxide isomer to hydrogen peroxide in the absence of metal complexation is only 3.7 kcal/mol.

Electronic Structure of Diamidoiron(III) Hydroperoxide. The reaction of hydrogen peroxide with ferric porphyrins is of particular interest to the peroxidases that catalyze the oxidation of a variety of compounds. Our objective in this study is not to specifically model the ferric porphyrin system because this is not yet feasible from a computational perspective at the *ab initio* level. Rather we wish to initially address the mechanism of the oxygen-transfer step involving an iron-bound hydroperoxide.

We have chosen the simplest diamido d^5-iron hydroperoxide (**7**) (Figure 4a) to initiate this *ab initio* study since its relative size is compatible with a sufficiently high level of theory to provide confidence in both the predicted geometry and energy. Initial calculations at the HF/3-21G level show that the sextet ($S = {}^5/_2$) is lower in energy than either a doublet or quadruplet spin state. The geometry of the iron atom prefers to be approximately tetrahedral, and constraining the N–Fe–N bond angle to 180° results in an energy increase of 31.6 kcal/mol. Prior calculations involving the O–O bond[9] have often pointed to the necessity for geometry optimization at a correlated level of theory. However, with this bridged iron hydroperoxide **7**, geometry optimization at the MP2 level gave an oxygen–oxygen bond distance (1.542 Å) that was identical to that found at the Hartree–Fock level (Table I).

To obtain a better description of the wave function for the bridged peroxo functionality in **7**, we have also optimized the geometry of **7** by employing the (14s, 11p, 6d, 1f)/[8s, 6p, 3d, 1f] basis set of Wachters and Hay (WH)[8] for the metal augmented with a 4f polarization function (Figure 4b). Both the O–O and proximal Fe–O_1 bonds are shortened with the larger basis set. A frequency calculation using analytical second derivatives at the HF/WH level established **7** to be a true minimum, and an SCF stability test confirmed the internal UHF stability of this high-spin bridged iron(III) hydroperoxide. The spin density on the iron atom is 4.82 electrons. The calculated value of S^2, 8.77, in **7** with both 3-21G and WH basis sets is in excellent accord with the expected $S^2 = 8.75$ for a sextet. We had experienced UHF stability problems with Fe=O and other simpler systems. Ironically, the number of lone pairs of electrons in **7** gives rise to a greater degree of d-orbital splitting and hence increased wave function stability. Full geometry optimization at the MP2 level with the WH basis set afforded a geometry that is surprisingly close to the HF/3-21G structure. At all levels of theory the Fe–OOH moiety is bidentate in nature with an Fe–O–O angle of 68.8–77.6° and a proximal Fe–O bond distance of ~1.9 Å with the second distal Fe···OH bond being ~2.1 Å (Table I). Isoelectronic density contour maps do not exhibit a bond critical

Table I. Optimized Geometries of Diamidoiron(III) Hydrogen Peroxide (**7**) at the Indicated Levels

	HF/ 3-21G	HF/ WH	MP2/ 3-21G	MP2/ WH	CASSCF(7,7)/ 3-21G
		Bond Lengths (Å)			
Fe–O_1	1.949	1.908	1.927	1.892	1.921
Fe–O_2	2.001	2.123	2.073	2.148	2.061
O_1–O_2	1.542	1.448	1.542	1.500	1.631
O_2–H_5	0.965	0.951	0.994	0.981	0.969
Fe–N_1	1.857	1.886	1.858	1.853	1.861
Fe–N_2	1.848	1.881	1.845	1.846	1.852
N_1–H_3	1.005	1.002	1.019	1.019	1.005
N_1–H_4	1.004	1.002	1.019	1.019	1.004
N_2–H_1	1.004	1.002	1.019	1.019	1.004
N_2–H_2	1.004	1.001	1.018	1.019	1.003
		Bond Angles (deg)			
Fe–O_1–O_2	68.8	77.1	72.4	77.6	70.4
O_1–O_2–H_5	105.7	104.5	101.4	100.6	99.2
N_1–Fe–N_2	122.8	122.2	123.3	122.5	122.6
H_1–N_2–H_2	109.9	109.3	110.3	109.9	109.5
H_3–N_1–H_4	109.6	109.1	110.0	109.5	109.8
		Dihedral Angles (deg)			
Fe–O_1–O_2–H_5	133.2	119.4	119.2	111.8	131.9
O_2–O_1–Fe–N_1	−103.1	−97.5	−99.0	−97.1	95.4
O_2–O_1–Fe–N_2	96.3	94.6	96.8	93.2	−100.7
O_1–Fe–N_2–H_1	−35.0	−12.8	−22.7	−8.1	−25.5
O_1–Fe–N_1–H_3	−24.6	−1.3	−37.9	−6.7	−25.9

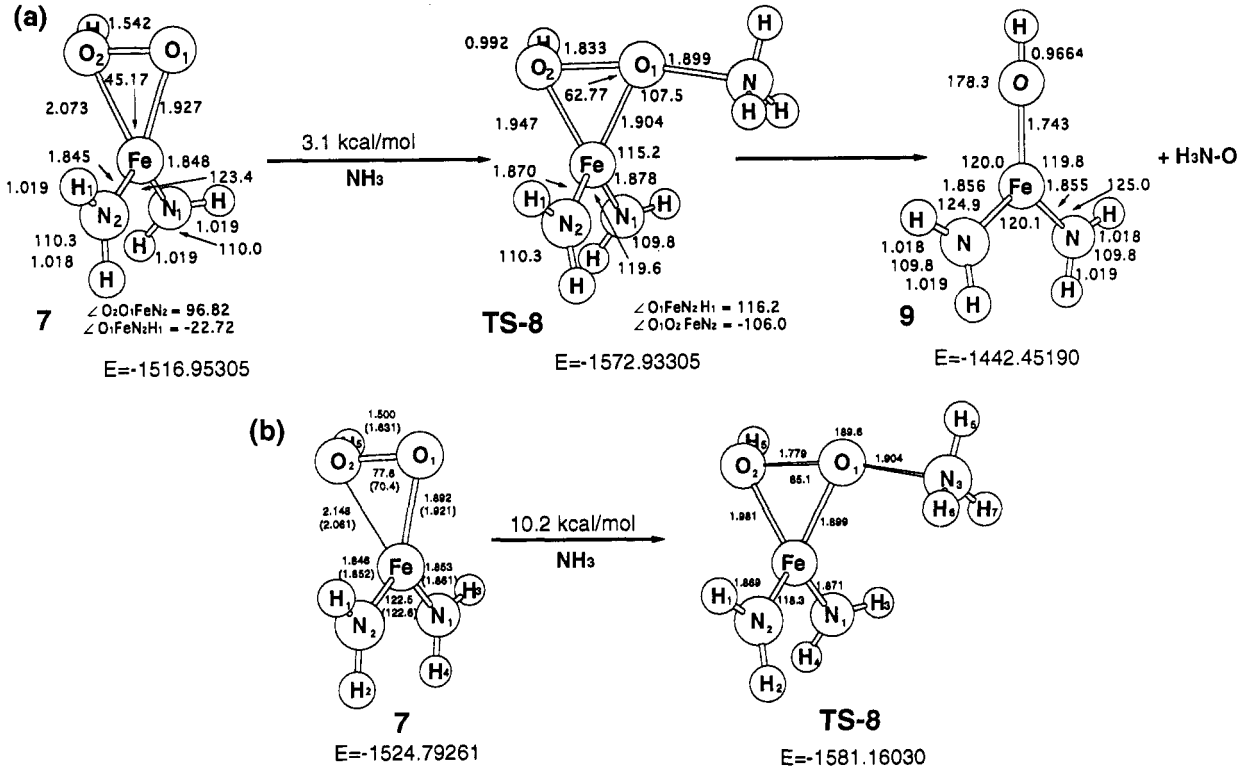

Figure 4. The optimized geometry of diamidoiron(III) hydroperoxide (7) and the transition structure (TS-8) for oxygen atom transfer from iron hydrogen peroxide: (a) optimized geometries and energies at the MP2/3-21G level and (b) geomeries optimized at MP2/WH and CASSCF(7,7)/3-21G (in parentheses) and energies at MP4//MP2/WH. Distances are given in Å, angles in deg, relative energies in kcal/mol, and total energies in au (E = -55.984 95 au for NH3 at MP2/3-21G and -56.383 95 au at MP4//MP2/WH).

point between Fe and the distal OH group, suggesting a secondary bonding interaction.

While iron hydroperoxide **7** exhibits a stable UHF wave function with both 3-21G and WH basis sets, dioxygen complexes of iron have been described as a singlet dioxygen, O_2 ($^1\Delta g$)σ donating to and accepting electron density from Fe^{2+}. The FeO_2 system is predicted to be a low-lying triplet state on the basis of generalized molecular orbital calculations (a limited MCSCF approach) with configuration interaction (CI).[12] Electron correlation must be introduced in order to obtain the correct ground state for FeO_2.

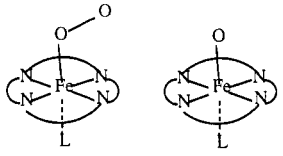

Evidence accumulated from X-ray data on model porphyrin systems suggests that the Fe–O–O bond angle in these dioxygen structures should be ~136°.[13] A multireference wave function is also essential for an adequate description of the electron structure and properties of ferryl oxygen model compounds. Complete active space SCF (CASSCF) calculations on the model iron–oxo–porphine depicted above indicate that the gross atomic spin population is nearly unity for both iron and oxygen.[5g]

The level of computation essential to adequately treat the above FeO_2 and Fe=O compounds raises concerns about the accuracy of single-reference wave functions for the iron hydroperoxides that we are examining. In order to assess the extent of electron transfer in both ground states and transition states involving the O–O bond, we typically perform a stability analysis of the wave function. In a number of instances involving O–O bond cleavage, we have found that the closed-shell description shows a modest RHF → UHF instability,[9] indicating that the wave function does not have sufficient flexibility to describe the molecule correctly. In the present case, these bridged iron hydroperoxides exhibit a stable UHF wave function and typically have essentially no spin contamination ($\langle S\rangle^2 = 8.77$). In order to provide more convincing evidence that the electronic structure of **7** is adequately described, CASSCF calculations were performed. The MP2/WH geometry was used to generate a set of UHF natural orbitals.[14] The UHF calculation showed the d-orbitals to be singly occupied, and all other doubly occupied orbitals had an orbital occupancy >1.99 electrons. The three lowest virtual orbitals had occupancies of 0.002–0.001 electrons. The orbital occupancy of the σ^*_{O-O} orbital is surprisingly low at 0.001 electrons. The UHF natural orbitals were used to start a CASSCF/3-21G geometry optimization on this sextuplet with the valence space consisting of the five d-orbitals and the σ and σ^* oxygen–oxygen orbitals (7 electrons, 7 orbitals). The predicted structure (Figure 4b) has an O–O bond elongation of 0.13 Å with all other variables being quite similar to those of the MP2/WH geometry. The O–O bond elongation with CASSCF geometry optimization was anticipated since we have previously found that the O–O bond in the TS for oxidation of ethane by water oxide (H_2O–O) was 0.3 Å longer than that predicted by the comparable geometry optimziation at the QCISD/6-31G* level.[15] In general we have suggested that dynamical correlation is far more important than nondynamical correlation with *both* the geometry and energetics of the peroxo functional group.[15] A CASSCF calculation on **7** with a larger active space that also included two oxygen lone pairs and a virtual p-orbital on iron (11 electrons, 10 orbitals) was also performed on the MP2/WH geometry. The value for the coefficient of the reference configuration (C_0) was 0.974, and the two virtual orbitals had 0.07 (σ^*_{O-O}) and 0.02 (σ^*_{Fe-O}) electrons each. From these

(12) Newton, J. E.; Hall, M. B. *Inorg. Chem.* **1984**, *23*, 4627.
(13) Jameson, G. B.; Molinaro, F. S.; Ibers, J. A.; Collman, J. P.; Brauman, J. I.; Rose, E.; Suslick, K. S. *J. Am. Chem. Soc.* **1980**, *102*, 3224.
(14) Hamilton, T. P.; Pulay, P. *J. Chem. Phys.* **1988**, *88*, 4926.
(15) Bach, R. D.; Andrés, J. S.; Su, M.-D.; McDouall, J. J. W. *J. Am. Chem. Soc.* **1993**, *115*, 5768.

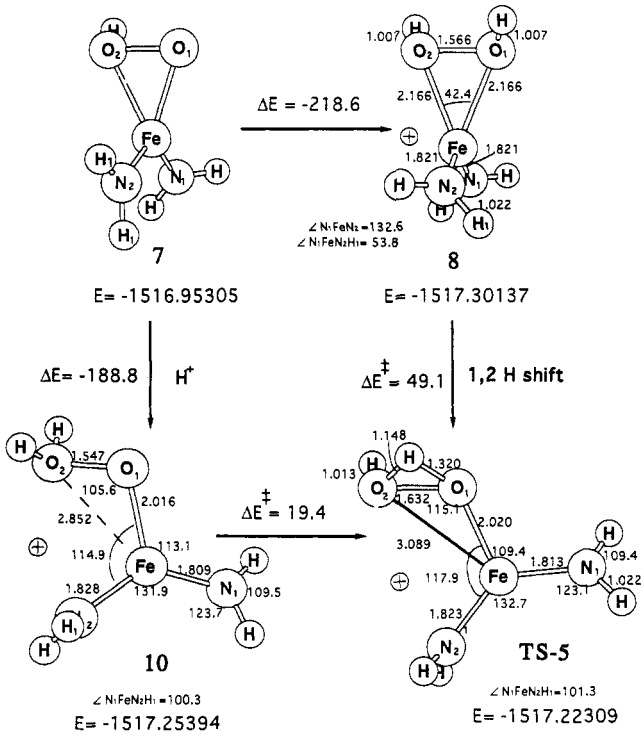

Figure 5. 1,2-hydrogen shifts in the protonated iron hydrogen peroxide cation calculated at the MP2/3-21G level. Distances are given in Å, angles in deg, relatives energies in kcal/mol, and total energies in au.

data we conclude that the single-reference MP2 approach is adequate to describe the ground-state wave function of this model iron hydroperoxide.

1,2-Hydrogen Shifts in Iron Hydroperoxide Cations. Although 1,2-hydrogen shifts in the lithium cations of hydrogen peroxide exhibit high activation barriers, it remains to be seen if the iron(III)-coordinated hydrogen peroxides behave in a similar manner. We have utilized second-order Møller–Plesset theory and a relatively small basis set for geometry optimization for this part of the study. The overall potential energy surfaces for the 1,2-hydrogen shifts in protonated diamidoiron(III) hydroperoxide (Figure 5) are remarkably similar to those noted above for the lithium complexes (Figure 3). The UHF wave function for TS-5 exhibited an internal UHF instability with the root = –0.07. Reoptimization of the molecular orbitals for this wave function resulted in an energy release of 5.6 kcal/mol. The iron(III) hydrogen peroxide complex **8** is 29.8 kcal/mol lower in energy than its isomeric water oxide complex **10**. However, the barrier height (TS-5) for a concerted 1,2-hydrogen shift from ground state **8** is 49.1 kcal/mol. The depths of the potential energy wells for the two water oxide metal complexes (H_2OO–Li^+ and H_2OO–$Fe^+(NH_2)_2$) relative to the heights of their transition states for reversion back to complexed hydrogen peroxide are comparable (Figure 1). We conclude from these data that the activation barriers for the 1,2-hydrogen shifts in the various cations of hydrogen peroxide do not differ significantly from that of hydrogen peroxide itself. The metal cations do serve to stabilize the metal complexes of water oxide to a sufficient extent that they could serve as potential oxygen donors. Because of the high barriers for a concerted 1,2-hydrogen shift, equilibrium between the isomeric forms of protonated hydrogen peroxide will almost certainly involve protonation–deprotonation or a proton relay mechanism.

Oxygen Atom Transfer from Metal Hydroperoxides. Oxygen atom transfer from hydrogen peroxide to ammonia has been studied at the MP2 level of theory. The reactive form of H_2O_2 in the gas phase is predicted to be water oxide (H_2OO) since the 1,2-hydrogen shift in H_2O_2 takes place prior to oxygen atom transfer. The barrier for H_3NO formation is predicted to be 54 kcal/mol.[9c] However, oxidation reactions involving alkyl hydrogen peroxides proceed by a pathway involving a 1,2-hydrogen transfer after the oxygen-transfer step.[9d]

Hydroperoxides are effective oxygen donors that can oxidize a variety of substrates. The mechanisms of these reactions are known to involve general acid catalysis.[16] Fully protonated hydrogen peroxide is also a highly reactive hydroperoxonium cation with a high propensity for the hydroxylation of a variety of substrates. Since a protonated iron hydroperoxide should exhibit similar reactivity, we have examined the relative reactivity of **7** and its protonated cation toward oxygen atom transfer. Employing the same protocol described above, we have first examined the reactivities of LiOOH and $LiOOH_2^+$ as oxygen donors (Figure 6). We elected to use ammonia as the nucleophilic substrate. The reactant cluster **11** derived from complexation of LiOOH + NH_3 is stabilized by 26.8 kcal/mol, and the transition state (TS-6) for the oxidation of ammonia is 48.3 kcal/mol above this reactant cluster (MP4//MP2/6-31G*). The relatively high activation energy reflects the nucleophilic character of both reactants.

The reactant complex between protonated lithium hydroperoxide (**6**) and ammonia is stabilized by 40.0 kcal/mol. However, the barrier height for oxygen atom transfer from this lithium cation of water oxide is reduced to 21.7 kcal/mol. In TS-7 (Figure 6), the water is being displaced as a neutral leaving group and the initial product of this S_N2-type displacement reaction is the lithium cation of ammonia oxide (NH_3OLi^+). As noted above, the hydrogen peroxide lithium cation (**5**) is the most stable form of metal-complexed hydrogen peroxide. The reactant cluster of **5** and ammonia (**13**) is stabilized by 47.7 kcal/mol (Figure 7). Consequently, a much higher barrier for oxygen transfer from **13** to ammonia (TS-8) is predicted (44.1 kcal/mol). Although TS-8 is 11.4 kcal/mol lower in energy than TS-7, the higher activation barrier for TS-7 is a direct result of the relative stabilities of the water oxide **12** versus the hydrogen peroxide **13** reactant structures of the oxygen atom donors (Figure 7). Since **5** is 26.1 kcal/mol more stable than **6**, at equilibrium, the relative concentration of the higher energy oxygen dono. would be insignificant.

Since the iron(III) system should in principle be a more effective oxygen donor than LiOOH, we next examined the relative reactivity of model iron hydroperoxide **7** in the oxidation of ammonia. The transfer of an oxygen atom from **7** to ammonia in a concerted manner should involve an S_N2 attack of NH_3 along the O–O bond with the formation of H_3N–O and diamidoiron(III) hydroxide (**9**). We calculated an activation barrier of 3.1 kcal/mol for TS-8 at the MP2/3-21G level of theory (Figure 4a). Attempts to locate TS-8 at the HF/WH level (Figure 4b) proved difficult because of an exceptionally long N–O bond distance (~2.44 Å). However, at the MP2/WH level, we observe an N–O bond distance (1.904 Å) that is quite consistent with our prior calculations on ammonia oxidation[9b] and comparable to that for oxidation with LiOOH (TS-6, first-order saddle point, MP2/6-31G*). We calculate a MP2/WH barrier of 15.6 kcal/mol, and at the MP4//MP2/WH level, TS-8 lies only 10.2 kcal/mol above its reactants (7 + NH_3). The displacement product for this oxygen transfer, $(H_2N)_2Fe$–OH, is also UHF stable at this level of theory. An analytical frequency calculation established that **7** (HF/WH and HF/3-21G) is a minimum and TS-8 (HF/3-21G) is a first-order saddle point.

We also have compared the relative reactivity of the model iron hydroperoxide to its protonated cation. The accepted mechanism for formation of a ferryl (Fe=O) oxygen donor, involving protonation of the distal oxygen of an iron hydroperoxide with the loss of H_2O (eq 1), prompted us initially to examine the

(16) (a) Dankleff, M. A. P.; Curci, R.; Edwards, J. O.; Pyun, H. *J. Am. Chem. Soc.* **1968**, *90*, 3204. (b) Ball, S.; Bruice, T. C. *J. Am. Chem. Soc.* **1980**, *102*, 6498.

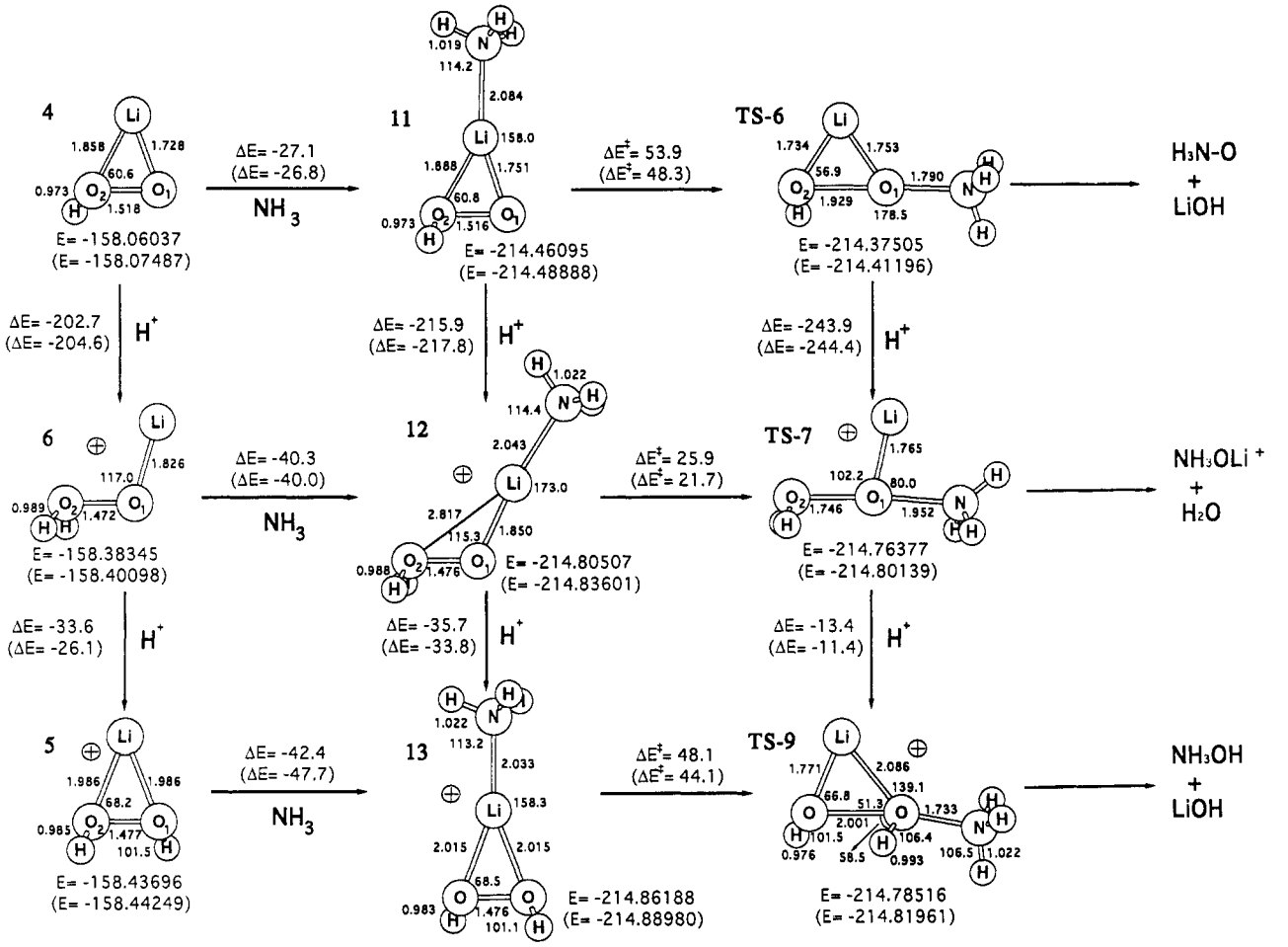

Figure 6. Reactant clusters and transition structures for oxygen atom transfer for lithium hydroperoxide (**4**), lithium-complexed water oxide (**6**), and lithium-complexed hydrogen peroxide (**5**) to ammonia calculated at the MP2/6-31G* level (MP4//MP2/6-31G* energies are in parentheses). Distances are given in A, angles in deg, relative energies in kcal/mol, and total energies in au. The energies for ammonia are -56.357 38 and -56.371 26 au.

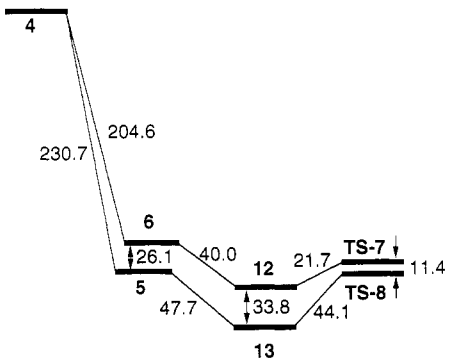

Figure 7. Relative energies (kcal/mol) at the MP4/6-31G*//MP2/6-31G *level* for the lithium cation complexes of H_2O_2 and H_2OO (**5**, **6**), the reactant clusters of **5** and **6** with ammonia (**13**, **12**), and the transition states for oxidation of ammonia (TS-8, TS-7).

structure and reactivity of protonated hydroperoxide **10**. Attempts at geometry optimization at both HF levels (3-21G and WH) did not lead to a stable energy minimum for **10**, and the molecule tended to dissociate with the loss of H_2O. However, at the MP2/3-21G level, we find an energy minimum for **10** but this protonated oxygen donor is no longer bridged and has an Fe–O_2 bond distance of 2.85 Å (Figure 5). The geometries calculated at the MP2/3-21G level for **7** and TS-8 are fortunately quite close to those obtained at MP2/WH (Figure 4). Partial optimization of both **10** and TS-10 at the higher MP2/WH level of theory also support this contention.

At the MP2/3-21G level, the activation barrier for the oxidation of ammonia by **7** (TS-8, Figure 4a) is 3.1 kcal/mol above its isolated reactants. By comparison, the transition structure (TS-10) for oxygen atom transfer from the water oxide form of protonated iron hydroperoxide **10** lies 37.8 kcal/mol below its isolated reactants (Figure 8).[17] Because of the computational time involved, we did not calculate the structure of the reactant clusters for either reaction. By comparison, the corresponding transition structure with the lithium cation (TS-7) was 18.3 kcal/mol lower in energy than its isolated reactants (Figure 6).

The iron hydroperoxide reaction profile closely parallels that predicted for the corresponding lithium hydroperoxides. The diamidoiron(II) complex with hydrogen peroxide (**8**) (Figure 8) is 29.8 kcal/mol more stable than the water oxide–iron cation **10**. The transition structure for oxygen atom donation from the more stable complex (TS-11) is 13.2 kcal/mol lower in energy than TS-10. The greater stability of **8** is also reflected in that fact that it lies only 11.8 kcal/mol below isolated reactants (**8** + NH_3).

Detailed experimental studies have recently provided a mechanistic rationale for general acid catalysis in the O–O bond cleavage step in cytochrome P-450 oxidation.[2c,d] These data strongly support a heterolytic O–O bond dissociation and are consistent with our earlier calculations on the marked effect of water catalysis on the reactivity of H_2O_2 and ROOH and on the efficacy of protonated hydrogen peroxide[9] as an oxygen donor. The present study suggests that protonated hydroperoxide **10** should also be a highly reactive intermediate that can undergo facile oxygen atom transfer prior to dissociation to a ferryl complex. These data also suggest that protonation of an iron

(17) The Fe–NH_2 rotational barriers in TS-10 are very small, making total geometry optimization at the MP2 level quite expensive. Since the changes in total energy were insignificant, geometry optimization was halted when all the RMS forces were less than 0.0004 au.

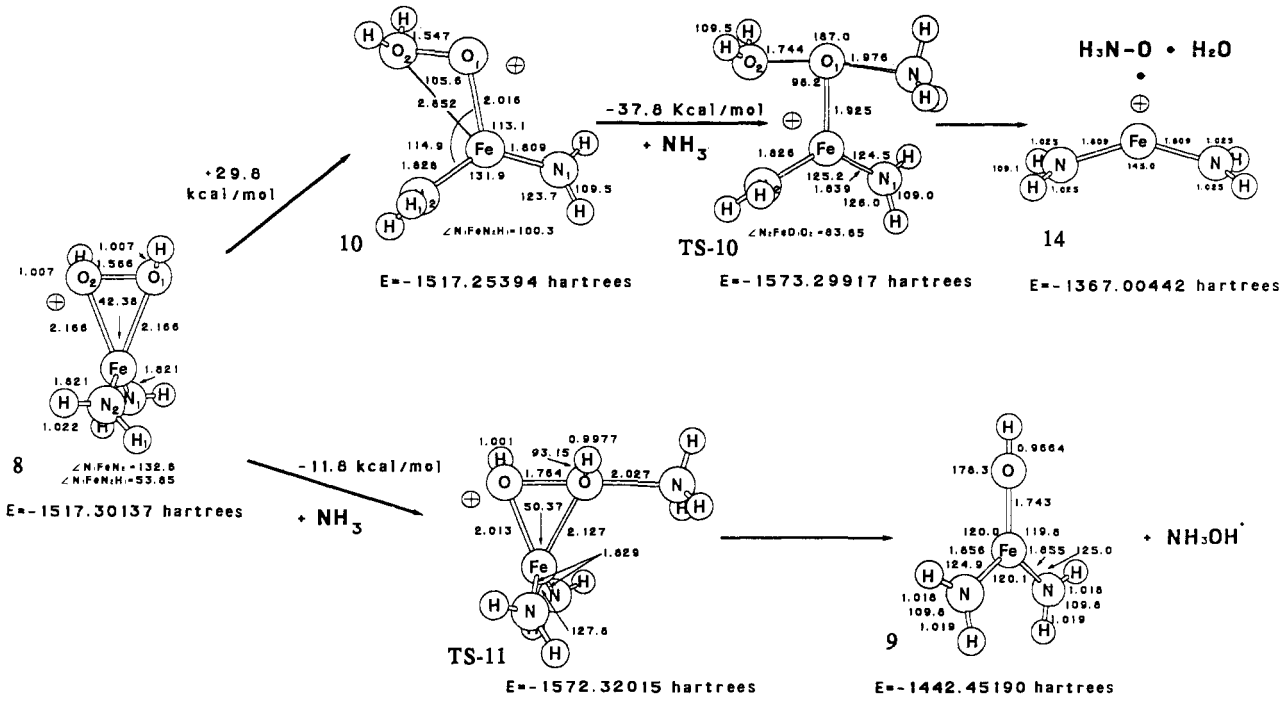

Figure 8. Optimized structures for the diamidoiron(II) complexes with hydrogen peroxide (**8**) and water oxide (**10**) and transition structures for oxygen atom transfer from protonated iron hydroperoxides to ammonia computed at the MP2/3-21G level. Distances are given in Å, angles in deg, relatives energies in kcal/mol, and total energies in au.

hydroperoxide on the distal oxygen, affording a water oxide structure resembling **10**, prior to loss of water, forming a ferryl oxygen, should be attended by a substantial increase in energy. This observation has serious implications concerning the accepted mechanism for loss of water from the protonated iron porphyrin hydroperoxide implicated in eq 1. However, at the active site, the energy difference between **8** and **10** could diminish by interactions with the surrounding protein since **10** has a higher dipole moment than **8**.

In summary, we have provided evidence that an iron(III) hydroperoxide is a bridged structure with the proximal Fe–O_1 bond only slightly shorter (0.26 Å) than that of the coordinated distal metal–oxygen bond. Oxygen atom transfer can be achieved by a 1,2-migration of the metal across the O–O bond that is symmetry allowed in both the σ and π planes of the O–O bond.[9b] The structure of this cyclic peroxo complex is further supported by excellent agreement between the experimental X-ray data[18] and our calculated (MP2/WH) bond lengths of 1.88 and 2.12 Å for the Ti–peroxo bonds in $(HO)_3Ti$–OOH. The intrinsic reactivity of **7** toward NH_3 is greater than that of LiOOH (TS-6, $\Delta E^{\ddagger}$ = 20.9 kcal/mol), and it is also a better oxygen atom donor than peroxyformic acid ($\Delta E^{\ddagger}$ = 16.5 kcal/mol).[9c] Although the highly abbreviated version of a protonated heme iron(III) hydroperoxide **10** has many shortcomings, it is an excellent oxygen donor, which suggests the possibility that in certain systems oxygen transfer could precede the formation of ferryl complex.

Acknowledgment. This work was supported in part by a grant from the National Science Foundation (CHE-90-20398), the National Institutes of Health (CA 47348-02), and the Ford Motor Company. We are very thankful to the Pittsburgh Supercomputing Center, Cray Research, and the Ford Motor Company for generous amounts of computing time. J.L.A. acknowledges the Spanish Ministerio de Educacion y Ciencia for financial support.

(18) Mimoun, H.; Chaumette, P.; Mignard, M.; Saussine, L. *Nouv. J. Chim.* **1983**, *7*, 467.